ISSN: 2319-5967
ISO 9001:2008 Certified
International Journal of Engineering Science and Innovative Technology (IJESIT)
Volume 7, Issue 1, January 2018

The Advantage of the Continuous Wavelet Transform over the Gabor Transform in Processing Signals with Rapidly Varying Amplitude

S.V.Bozhokin, I.B.Suslova, D.E.Tarakanov

Abstract*— The comparison of the Gabor and wavelet transforms is based on the simulation of nonstationary signals (NS) as a superposition of specially composed elementary signals (ENS). The model proposed by the authors leads to the superposition signal with rapidly varying in time amplitude. In the framework of the given model both the Gabor (GT) and continuous wavelet transforms (CWT) can be calculated analytically. CWT uses the Morlet mother wavelet function with a control parameter, which changes the spectral resolution of the signal. The criteria for matching the signal and its power spectrum behavior with the corresponding GT and CWT images are introduced. The study shows the advantages of CWT, which adapts the window to the signal, over GT, which requires extra efforts and information to specify the window size.

***Index Terms*— Gabor transform, nonstationary signal, wavelet transform.**

I. INTRODUCTION

The problem of the most effective method for processing non-stationary signals is still the subject of scientific discussion. Spectral and statistical properties of a large number of non-stationary (*NS*) signals $Z(t)$, which occur in physics, biology and medicine, vary in time [1-6]. The Fourier transform (*FT*) allows us to detect the presence of different harmonics $Z(\nu)$ with frequency ν in the signal $Z(t)$, but not to trace their appearance and disappearance in time. If we are to find the spectral composition of a signal varying in time, instead of integrating over the whole time interval $-\infty < t < \infty$, we may consider a certain finite interval W [t–W/2,t+W/2] and calculate *FT* over this interval. Then we shift the window and repeat the procedure. Thus, we can study how the signal spectral properties vary in time. Such a windowed *FT* called *STFT* (Short-time Fourier transform) in the case of the window having the Gaussian form is referred to as the Gabor transform (*GT*) [7-8].

The drawback of *GT* is that its form and results depend heavily on the window size. To choose the optimal window length W we need additional information about the time-scales in which spectral rearrangements occur. It is known that a wide window gives good resolution in frequency, but bad resolution in time. A very wide window is suitable for detecting low frequency signal components but will be excessive in detecting high frequency harmonics. More recently, the theory of continuous wavelet transform (*CWT*) has become a new approach in the study of *NS* processes [9-10]. The form of *CWT* depends on the choice of the mother wavelet function, which works as an adaptive window adjusting the resolution in both time and frequency. The comparison of *GT* and *CWT* by numerical methods [11-18] showed that for many signals strongly varying in time the choice of the window size for an adequate description of *NS* turned out a difficult problem.

The purpose of the paper is to compare *GT* and *CWT* based on the developed model of *NS* with the amplitude rapidly varying in time and the analytical solution of the transformation problem. Within the framework of the model, we can specify the amplitude and frequency properties of the signals and check the results analytically. To optimize the use of *CWT* (for the best resolution in both time and frequency) we include the control parameter m [19] into the Morlet mother wavelet function.

ISSN: 2319-5967
ISO 9001:2008 Certified
International Journal of Engineering Science and Innovative Technology (IJESIT)
Volume 7, Issue 1, January 2018

II. METHODS

A. *Simulation of non-stationary signal*

We assume non-stationary (*NS*) signal $Z(t)$ to be the superposition of elementary non-stationary (*ENS*) signals centered in $t = t_L$

$$Z(t) = \sum_{L=0}^{N-1} z_L(t - t_L). \tag{1}$$

Each *ENS* in (1) is a product of the Gaussian envelope on oscillating function [20-21]:

$$z_L(t - t_L) = \frac{b_L}{2\sqrt{\pi}\tau_L} \exp\left(-\frac{(t - t_L)^2}{4\tau_L^2}\right) \cos\left[2\pi f_L(t - t_L) + \alpha_L\right], \tag{2}$$

where f_L is the frequency of oscillations (*HZ*); t_L is the center of the signal localization (*s*); τ_L is the characteristic size of the signal localization in time (*s*); α_L is the initial phase in radians; b_L is the amplitude of *ENS*.

Let us assume that the frequencies of all *ENS* in (1) are equal $f_L = f_0$, whereas the times t_L and phases α_L (L>0) are related to the parameters t_0 and α_0 by the formula

$$2\pi f_0(t_0 - t_L) + \alpha_L - \alpha_0 = 2\pi n, \tag{3}$$

where n=0,±1,±2,±3…. . It follows that we can represent the signal of superposition $Z(t)$ as

$$Z(t) = B(t)\cos\left[2\pi f_0(t - t_0) + \alpha_0\right]. \tag{4}$$

The value of $B(t)$ is given by

$$B(t) = \frac{1}{2\sqrt{\pi}} \sum_{L=0}^{N-1} \frac{b_L}{\tau_L} \exp\left[-\frac{(t - t_L)^2}{4\tau_L^2}\right]. \tag{5}$$

Consider the model (4)-(5), for which the coefficients may have different signs leading to different signs in $B(t)$. We introduce the concept of the positive amplitude as

$$A(t) = |B(t)|. \tag{6}$$

As an example, consider $Z(t)$ (1) be the sum of four *ENS* (L = 0,1,2,3). Let all the frequencies be equal $f_L = f_0$=2.5 *Hz*, and all the phases have zero values $\alpha_L = \alpha_0$=0. The other parameters of the *ENS* are shown in Table 1. They satisfy the equation (3).

Table 1. The parameters of four *ENS* (1)

L	b_L (s)	t_L (s)	τ_L (s)
0	20	12	3
1	-30	16	2
2	25	20	1
3	-20	22	0.5

Time behavior of $Z(t)$ is given in Fig.1.

ISSN: 2319-5967
ISO 9001:2008 Certified
International Journal of Engineering Science and Innovative Technology (IJESIT)
Volume 7, Issue 1, January 2018

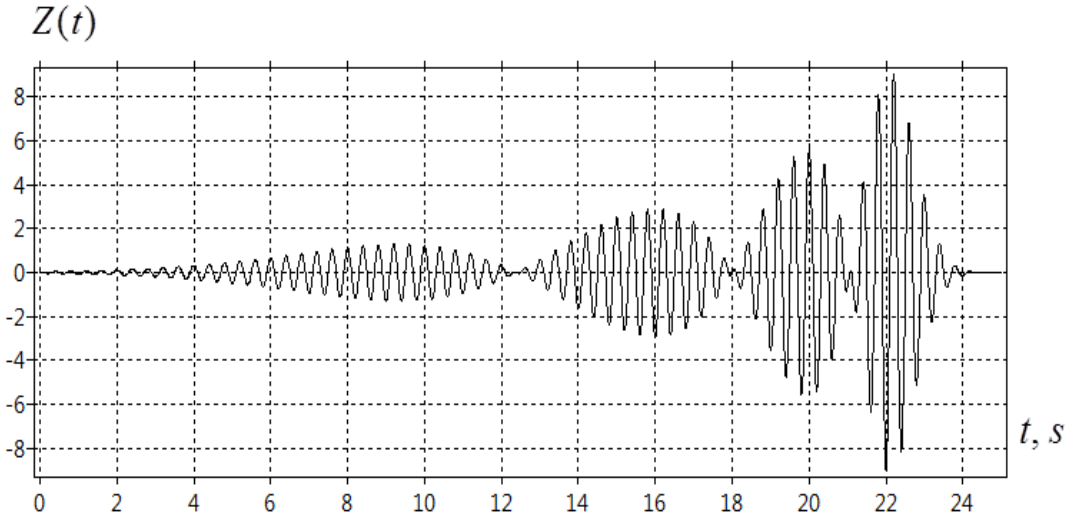

Fig. 1. Time behavior of $Z(t)$.

The rapidly varying amplitude $A(t)$ is zero at time moments t ={12.4 *s*; 18.0 *s*; 21.0 *s*}.

B. GT and CWT of non-stationary signals

GT [4, 7, 16] with the parameter *W* (the size of the window) is widely used to process non-stationary signals. The Gabor transform uses functions $\chi_W(\nu,t)$, which are the product of harmonics $\exp(-2\pi i\nu t)$ with the frequency ν (*Hz*) and a real function of the Gaussian window $R_W(t)$ having a characteristic dimension *W*, i.e.

$$\chi_W(\nu,t) = R_W(t)\exp(2\pi i\nu t), \tag{7}$$

$$R_W(t) = \frac{1}{\sqrt{W\sqrt{2\pi}}}\exp\left(-\frac{t^2}{4W^2}\right). \tag{8}$$

The Gaussian window function has a unit norm. The duration of the Gaussian window in time equals $\Delta_t = W$, while its extension along the frequency axis is $\Delta_\nu = 1/(4\pi W)$. The Gabor transform

$$g_W(\nu,t) = \int_{-\infty}^{\infty} Z(t')\chi_W^*(\nu,t'-t)\,dt' \tag{9}$$

represents the convolution of signal $Z(t)$ with the complex conjugation of $\chi_W(\nu,t)$. The center of the window is at the point $t = t'$. By moving the window center along t' - axis ($t - W < t' < t + W$), we can follow the change in the frequency composition of signal $Z(t')$ within the window. The analogue of the Parseval equality for *GT* and the formula for the inverse transformation that allows us to reconstruct the signal from its *GT* transform (9) are given in [4].

Analytical formulas of the Gabor transform $g_W^{(L)}(\nu,t)$ applied to the signal (2) in relation to frequency ν (*Hz*) and time t (*s*) are given in [21]. Superposition principle allows us to obtain the Gabor transform $g_W(\nu,t)$ (9) of the complex signal (1). The two-dimensional surface $|g_W(\nu,t)|$ at W =0.2 *s* is given in Fig.2. It tracks the time behavior of $A(t)$ with the maximum at $\nu = f_0$.

ISSN: 2319-5967
ISO 9001:2008 Certified
International Journal of Engineering Science and Innovative Technology (IJESIT)
Volume 7, Issue 1, January 2018

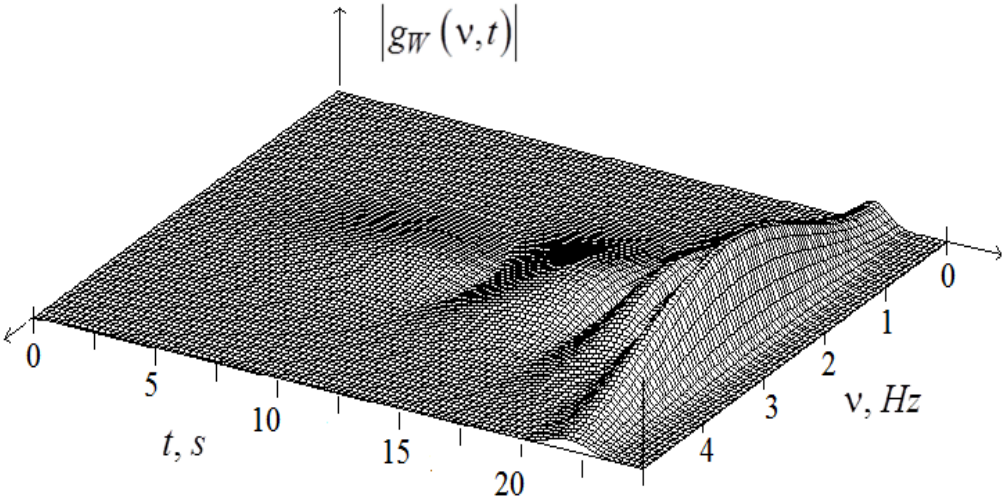

Fig. 2. ***GT*** **of** $Z(t)$ **(1) in relation to frequency** ν **(*Hz*) and time** t **(s) for** W **=0.2 *s*.**

For small windows $1/(f_L\tau_L) << W/\tau_L << 1$, *GT* tracks the form of the amplitude. However, the frequency correlation between *GT* of *ENS* and its power spectrum is small. We should note that for correct display of the signal with *GT*, it is necessary to ensure that several oscillation periods T_L ($T_L = 1/f_L$) be placed within the window size, i.e. $1/f_L << W$. *GT* with wide window does not track the form of the amplitude, but fits well with the power spectrum. For *NS* signal (1), which represents the superposition of *ENS* with different value of τ_L (Table 1), the choice of window size becomes a separate problem.

Let us introduce the criteria for the correct correspondence of $g_W(\nu,t)$ (9) behavior to the signal properties.

$$\sigma_t^2(\mathrm{GT}) = \frac{1}{T}\int_0^T \left[\frac{A^2(t)}{A^2_{\max}(t_{\max})} - \frac{|g_W(f_0;t)|^2}{|g_{W\max}(f_0;t)|^2} \right]^2 dt, \qquad (10)$$

$$\sigma_\nu^2(\mathrm{GT}) = \frac{1}{F_{\max}}\int_0^{F_{\max}} \left[\frac{P(\nu)}{P_{\max}(\nu_{\max})} - \frac{|g_W(\nu;t_0)|^2}{|g_{W\max}(\nu,t_0)|^2} \right]^2 d\nu, \qquad (11)$$

where $\sigma_t(GT)$ is the standard deviation showing how the amplitude $A(t)$ (6) normalized to its maximum value differs from the time behavior of $|g_W(f_0,t)|$ normalized to its maximum value; $\sigma_\nu(GT)$ is the standard deviation showing how the power spectrum $P(\nu)$ normalized to its maximum value $P_{\max}(\nu_{\max})$ differs from the $|g_W(\nu,t_0)|$ (as a function of frequency) normalized to its maximal value $|g_{W\max}(\nu,t_0)|$. The fixed parameters in (7)-(8) include the period of observation T=25 *s*; the frequency f_0=2.5 *Hz*; the upper limit of frequency $F_{\max}$=10 *Hz*; the moment of time $t_0 = T/2$. Criteria (10)-(11) determine how accurately *GT* tracks spectral and temporal behavior of non-stationary signal $Z(t)$ (1).

Currently, the continuous wavelet transform (*CWT*) [4, 9, 10, 22, 23] is widely used in processing *NS* signals. Continuous wavelet transform $V(\nu,t)$ (*CWT*) maps the non-stationary signal $Z(t)$ with varying time-frequency structure on time-frequency plane

ISSN: 2319-5967
ISO 9001:2008 Certified
International Journal of Engineering Science and Innovative Technology (IJESIT)
Volume 7, Issue 1, January 2018

$$V(\nu,t)=\nu\int_{-\infty}^{\infty}Z(t')\psi^{*}\left(\nu(t-t')\right)dt', \tag{12}$$

where $\psi(x)$ is the mother wavelet function; symbol * means complex conjugation. The value of frequency $\nu>0$ determines the scale of compression or stretching of the mother wavelet along the time axis. The argument t shows the position of the wavelet center on the time axis. The mother wavelet $\psi(x)$ should be localized near the point $x=0$, have unit norm, and zero mean value calculated over the total interval $-\infty< x <\infty$. The adaptive Morlet mother wavelet function (*AWM*), which we introduced in [19], satisfies all these properties. The formulas for *AMW* and its Fourier image are

$$\psi(x)=D_m\exp\left(-\frac{x^2}{2m^2}\right)\left[\exp(2\pi ix)-\exp\left(-\Omega_m^2\right)\right], \tag{13}$$

$$\hat{\psi}(F)=\frac{D_m\Omega_m}{\sqrt{\pi}}\exp\left[-\Omega_m^2(F-1)^2\right]\left[1-\exp\left(-2\Omega_m^2F\right)\right], \tag{14}$$

$$D_m=\frac{(2\pi)^{1/4}}{\sqrt{\Omega_m\left(1-2\exp\left(-\frac{3\Omega_m^2}{2}\right)+\exp\left(-2\Omega_m^2\right)\right)}}\ . \tag{15}$$

The value m in (13)-(15) plays the role of a control parameter, and $\Omega_m=m\pi\sqrt{2}$. The parameters of localization Δ_x [1, 4], which indicates the extension of $\psi(x)$ along the x-axis, and Δ_F, which corresponds to the extension of Fourier spectrum $\hat{\psi}(F)$ [1,4] along the frequency axis, have the values $\Delta_x\approx m/\sqrt{2}$, and $\Delta_F\approx 1/(\sqrt{8}\pi m)$. Their product $\Delta_x\Delta_F=1/(4\pi)$ is close to the lowest value. The values of Δ_x and Δ_F can vary with the change in m. Thus, we get the opportunity to vary the time and spectral resolution of the signals under study. At m =1 we obtain the formula for the ordinary Morlet wavelet function.

If the characteristic length of $\psi(x)$ is $\Delta_x\approx m/\sqrt{2}$, then the characteristic time moments, which make the main contribution to the integral (7), satisfy the relation

$$t-\frac{\Delta_x}{\nu}<t'<t+\frac{\Delta_x}{\nu}\ . \tag{16}$$

Thus, *AMW* (8) behaves as a varying window depending on the control parameter. The window width automatically becomes large for small frequencies and small for large ones (16).

The analytical expression for wavelet transform $V_L(\nu,t)$(12) of *ENS* (2) with the control parameter *m* in the Morlet mother wavelet function is given in [19].This parameter changes both spectral and amplitude resolution of the signals under study. Fig.3 shows wavelet transform of $Z(t)$ (1) at $m=1$. *CWT* formulas for $\sigma_t(CWT)$ and $\sigma_\nu(CWT)$ can be obtained by replacing $|g_W(\nu,t)|$ (9) by $|V(\nu,t)|$ (12) in (10)-(11). Note that both *CWT* at $m=1$ (Fig.3) and *GT* at W =0.2 *s* (Fig.2) are good enough to describe the behavior of $A(t)$. However, frequency distribution of *CWT* is much better localized.

ISSN: 2319-5967
ISO 9001:2008 Certified
International Journal of Engineering Science and Innovative Technology (IJESIT)
Volume 7, Issue 1, January 2018

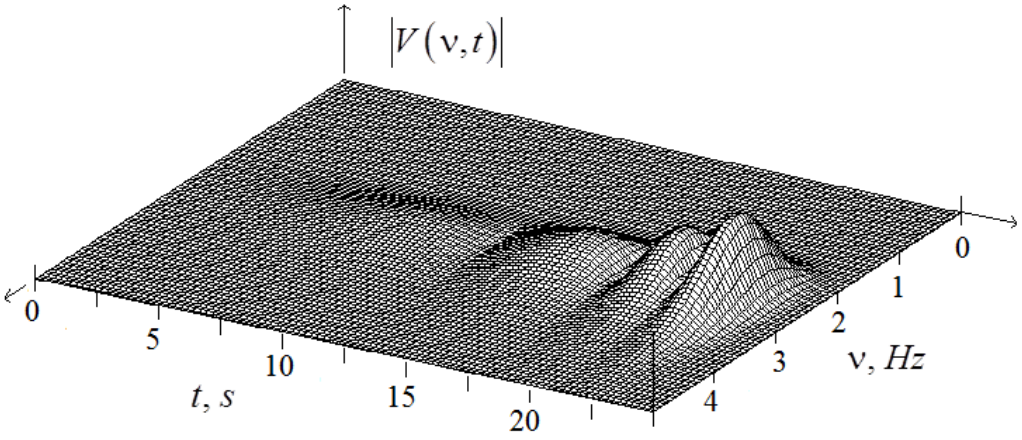

Fig. 3. $|V(\nu,t)|$ **of signal** $Z(t)$ **(1) depending on frequency** ν **,** ***Hz*** **and time** t **,** ***s*** **at** $m=1$.

C. Results and Discussion

Let us compare the time behavior of signal amplitude $A(t)$, $|g_W(f_0,t)|$ (*GT*) and $|V(f_0,t)|$ (*CWT*) at fixed frequency f_0 =2.5 *Hz* (Fig.4). *GT* and *CWT* are normalized at their maximum values $|g_{W\max}|$ and $|V_{\max}|$. We consider the interval t = [12 *s*, 25 *s*], where zeroes of $A(t)$ are localized. The optimal values W =0.2 and $m=1$ were obtained in numerous *GT* and *CWT* calculations with the parameters of these transforms varying by small step in the range *W*= [0.025 *s*; 20 *s*] and m = [1; 100].

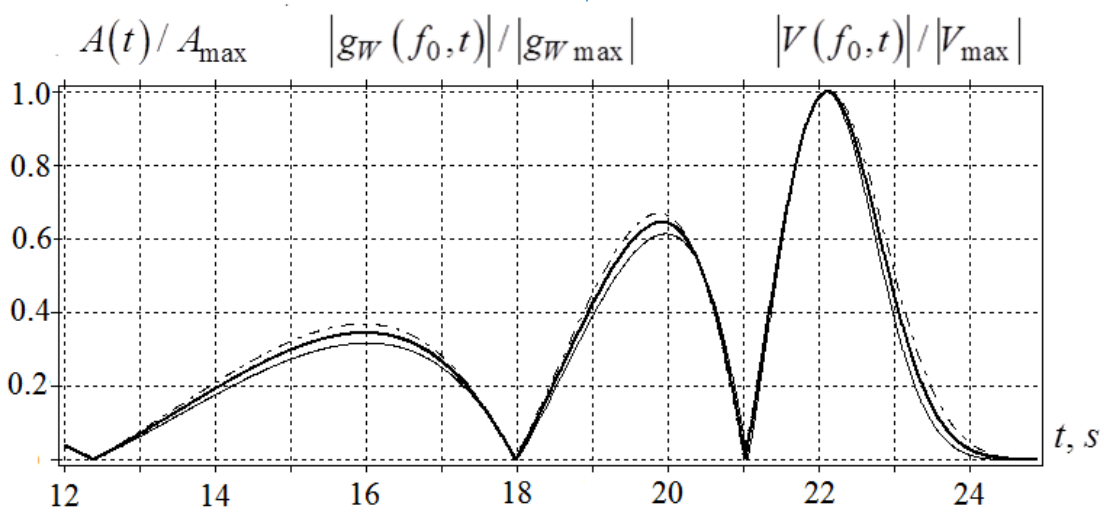

Fig. 4. Thin line – the signal amplitude $A(t)$ **(6); bold line – normalized** ***GT*** **of the signal at fixed frequency** f_0 **=2.5** ***Hz*** **and** W **=0.2** ***s*****; dash-dot line –normalized** ***CWT*** **at fixed frequency** f_0 **=2.5** ***Hz*** **and** m **=100.**

The joint behavior of four *ENS* (Table1) results in the appearance of two narrow peaks near the frequency f_0 =2.5 *Hz* in the signal power spectrum plot $P(\nu)=|Z(\nu)|^2$, where $Z(\nu)$ is the Fourier transform of $Z(t)$. The question is whether *GT* and *CWT* can reproduce such a picture. We compare the spectral distributions (Fig.5) in the narrow frequency range ν =[2 *Hz*, 3 *Hz*], where this structure is vividly expressed.

ISSN: 2319-5967
ISO 9001:2008 Certified
International Journal of Engineering Science and Innovative Technology (IJESIT)
Volume 7, Issue 1, January 2018

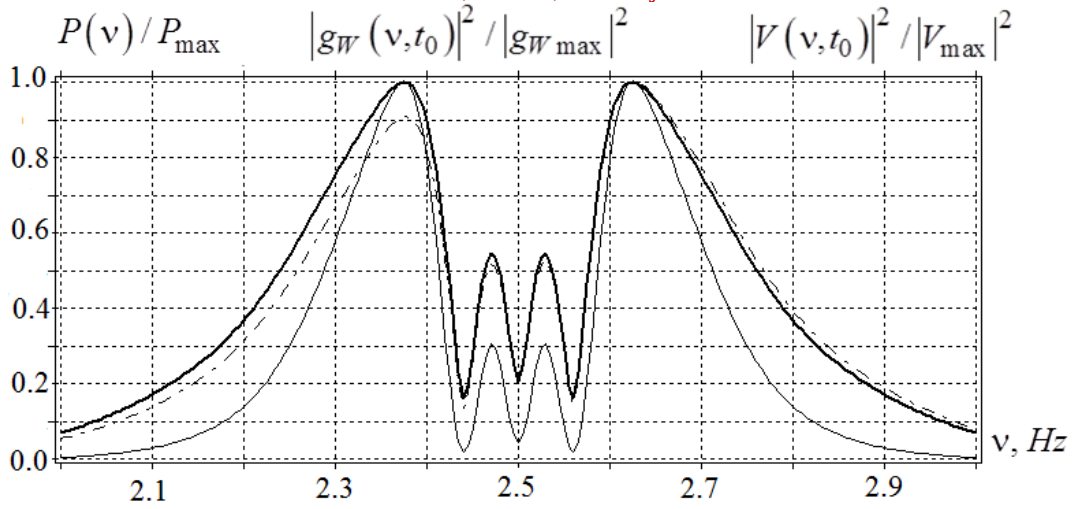

Fig. 5. The thin line denotes the power spectrum $P(\nu)$ of (1); bold line, the normalized *GT* of the signal at fixed t_0 =13 *s* and W =20 *s*; the dash-dot line shows normalized *CWT* at fixed t_0 =13 *s* and m =100.

The analysis of curves in Fig.5 shows that *GT* (at $W/\tau_{\max} >> 1$) and *CWT* (at $m >> f_0\tau_{\max}$), where $\tau_{\max}$ is the maximal value of τ_L (Table1), track the complex behavior of $P(\nu)$ well.

Fig.6 shows the dependence of $\sigma_t(GT)$ on non-dimensional argument $x = W/\tau(1)$ at $\tau(1)$ =1 *s* and the dependence of $\sigma_t(CWT)$ on the parameter $x = m$ (*m* is the control parameter in the Morlet mother wavelet function) (bold line). The graph corresponding to *GT* (thin line) has the minimum at $W \approx 0.2$ *s*. The value $\sigma_t(CWT)$ (bold line) increases in the range $1 \le m \le 10$ monotonically with increasing $x = m$. For *GT* and *CWT*, the graphs in Fig.6 show approximately the same minimal values $\sigma_{t\min}(GT) \approx 0.02$ (W =0.2 s) and $\sigma_{t\min}(CWT) \approx 0.03$ (m =1). However, in the case of *GT*, we observe a very narrow segment corresponding to minimal values of σ_t in the vicinity of the optimal value of the window length W =0.2 *s* (Fig.2,4,5). For *CWT*, you do not need to search for the optimal window size. Setting the control parameter m =1, we automatically achieve a very good tracing of signal $A(t)$ with the help of *CWT*.

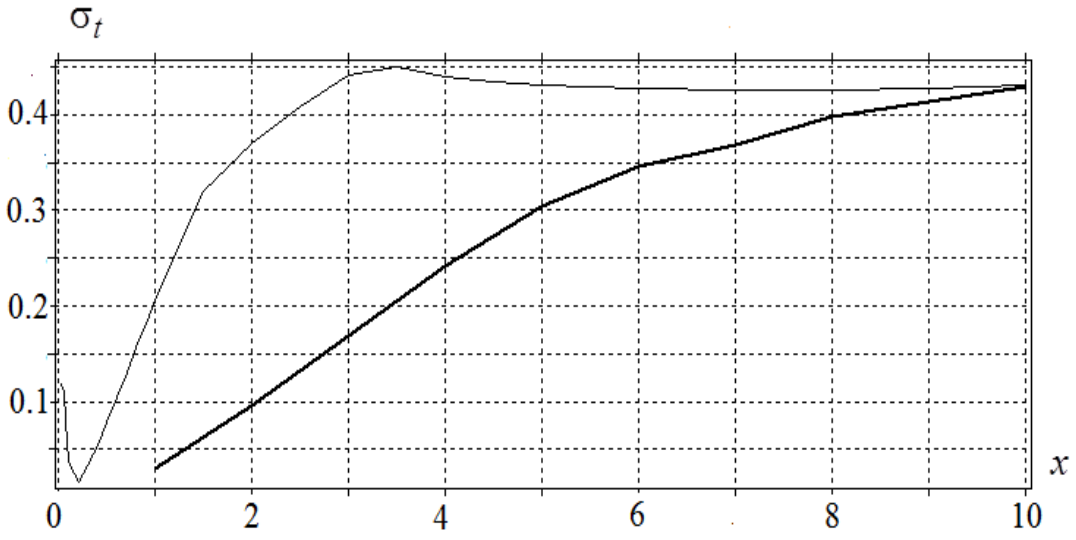

Fig. 6. $\sigma_t(GT)$ Depending on $x = W/\tau(1)$ (thin line) and $\sigma_t(CWT)$ depending on $x = m$ (bold line).

ISSN: 2319-5967
ISO 9001:2008 Certified
International Journal of Engineering Science and Innovative Technology (IJESIT)
Volume 7, Issue 1, January 2018

Similar calculations can be made for $\sigma_\nu(GT)$ at different window size (W) values and for different control parameter (m) values. The results are shown in Fig.7.

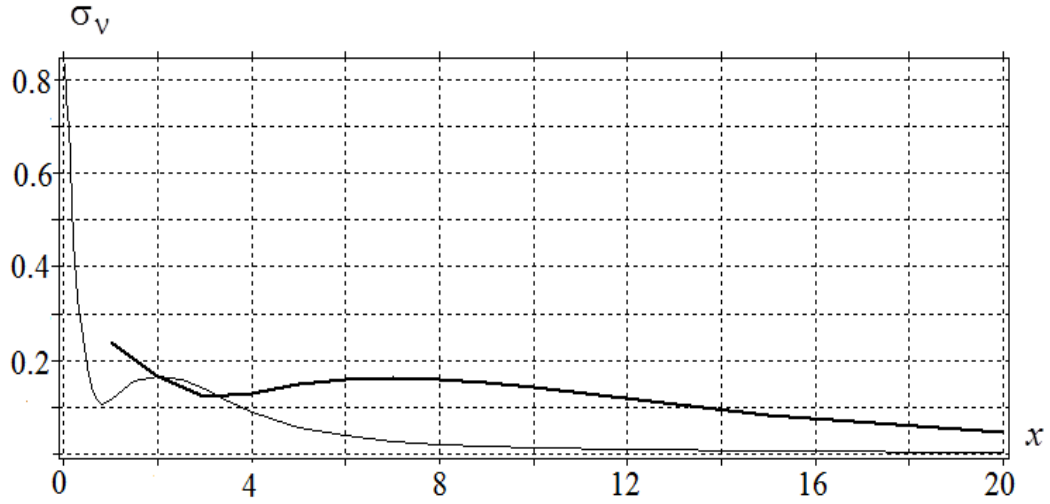

Fig. 7. $\sigma_\nu(GT)$ **depending on** $x = W/\tau(1)$ **(thin line) and** $\sigma_\nu(CWT)$ **depending on** $x = m$ **(bold line).**

In fact, at small $x << 1$, we can reconstruct the power spectrum $P(\nu)$ of the complex signal neither by using *GT* ($|g_W(\nu;t_0)|^2$) nor *CWT* ($|V(\nu,t_0)|^2$), t_0 =13 *s*. However, the value $\sigma_\nu(GT) \approx 0.45$ at optimal window size $W \approx 0.2$ is larger than $\sigma_\nu(CWT) \approx 0.24$ at m =1. For *GT* with large window $W \approx T/2$ and *CWT* at $m >> f_0\tau_{\max}$, the values σ_ν are small, i.e. $\sigma_\nu(GT)$ =0.003 at W =20 s, and $\sigma_\nu(CWT) \approx 0.02$ at $m = 100$. This means that for such parameter values, *GT* and CWT give good approximation of power spectrum $P(\nu)$.

It should be noted that the reconstruction of the power spectrum of a complex non-stationary signal with strongly varying amplitude-frequency properties is rather an academic problem. In the processing of non-stationary signals, it is more important to determine time variation of frequency spectrum. *CWT* at $m = 1$ and with the window changing its size with frequency manage this task automatically. In the case of the signals with a large spread in frequencies f_L and characteristic values τ_L, the use of *GT* encounters considerable difficulties. The reason is that the proper approximation of the amplitude $A(t)$ with *GT* requires fulfilling the inequality $1/f_L << W << \tau_L$. If the signal represents the superposition of *ENS* with different values of f_L and τ_L, the choice of optimal W satisfying all the ENS becomes impossible.

III. CONCLUSION

We proposed a model of non-stationary signal with prescribed complex dependence on the time of amplitude and spectral characteristics. For this model, the Gabor transform (*GT*) and continuous wavelet transform (*CWT*) were calculated analytically and compared. In the calculations, we varied the window size W (*GT*) and the control parameter m in the mother wavelet function (*CWT*). The main advantage of *CWT* over *GT* is that applying *CWT* with $m = 1$, you can at once determine correctly the signal amplitude $A(t)$ as a function of time, while in the case of *GT* you should first solve the problem of choosing the optimal window size.

The results of the work can be applied in testing numerical problems in the study of signals with complex amplitude and frequency properties; in analyzing flares in astrophysics, in seismology, encephalography, cardiography, and in interpreting the parameters of optical media irradiated by femtosecond lasers.

ISSN: 2319-5967
ISO 9001:2008 Certified
International Journal of Engineering Science and Innovative Technology (IJESIT)
Volume 7, Issue 1, January 2018

ACKNOWLEDGMENT

The work was carried out under the support of Russian Scientific Foundation (the project N 17-12-01085).

REFERENCES

[1] C.K.Chui, "An Introduction to Wavelets", Academic Press, New York, 1992.

[2] A.E.Hramov, A.A.Koronovskii , V.A. Makarov, A.N.Pavlov, E.Sitnikova, "Wavelets in neuroscience", Springer Series in Synergetics, Springer-Verlag, Berlin, Heidelberg., 2015.

[3] I.Daubechies., "Ten lectures on wavelets", Philadelphija: SIAM, 1992.

[4] S.A.Mallat, "A Wavelet Tour of Signal Processing", 3rd ed., Academic Press, New York, 2008.

[5] A.Cohen, "Numerical Analysis of Wavelet Method", North-Holland, Elsevier Science, 2003.

[6] "Advances in Wavelet Theory and Their Applications in Engineering, Physics and Technology". Edited by Dumitru Baleanu, 2012.

[7] D.J. Gabor, "Theory of Communication", J. Inst. of Elect. Eng. Part III, Radio and Communication, vol.93, pp. 429-457. 1946.

[8] P.Goupillaud, A.Grossmann, J. Morlet, "Cycle-octave and related transforms in seismic signal analysis", Geoexploration, Vol.23, pp.85-102, 1984.

[9] C.K.Chui, O.Jiang, "Applied Mathematics. Data Compression, Spectral Methods, Fourier Analysis, Wavelets and Applications", Mathematics Textbooks for Science and Engineering, Atlantis Press, Vol.2, 2013.

[10] P.S.Addison, "The illustrated wavelet transform handbook. Introductory theory and application in Science, engineering, medicine and finance", Second Edition, CPC Press. 2017.

[11] S.Dass, M.S. Holi, K.S. Rajan, "A Comparative Study on FFT, STFT and WT for the Analysis of Auditory Evoked Potentials", International Journal of Engineering Research and Technology (IJERT), Vol.2 no 11, pp. 636-641, 2013.

[12] S.H.Cho, G.Jang, S.H. Kwon, "Time-Frequency Analysis of Power-Quality Disturbances via the Gabor-Wigner Transform", IEEE Transaction on Power Delivery, Vol. 25, no 1, pp. 494-499, 2010.

[13] M.Szmajda, K.Górecki, J.Mroczka, Metrol. "Gabor transform, SPWVD, Gabor-Wigner transform and wavelet transform - tools for power quality monitoring", Meas. Syst., Vol. 17, no 3, pp.383-396, 2010.

[14] E. Shokrollahi, G.Zargar, M.A.Riahi, "Using continuous wavelet transform and short time fourier transform as spectral decomposition methods to detect of stratigraphic channel in one of the Iranian south-west oil fields", Int. J. Sci. Emerging Tech., Vol. 5, no 5, pp. 291-299, 2013.

[15] R.RYadav, D.J.Sanghvi, "QRS complex detection using wavelet transform", International Journal of Engineering Science and Innovative Technology (IJESIT), V.2, N3, pp.290-293, 2013.

[16] E.D.Ubeyli, I.Guler, "Spectral broadening of ophthalmic arterial Doppler signal using STFT and wavelet transform", Computers in Biology and Medicine, Vol.34, pp. 345-354, 2004.

[17] L.Cnockaert, P.F.Migeotte, L.Daubigny, G.K.Prisk, F.Grenez, R.C.Sa, "A method for the analysis of respiratory sinus arrhythmia using continuous wavelet transforms", IEEE Transactions on biomedical engineering, Vol. 55, no 5, pp. 1640-1642, 2008.

[18] T.M.E.Nijsen, R.M.Aarts, P.J.M.Cluitmans, P.A.M.Griep, "Time-frequency analysis of accelerometry data for detection of myoclonic seizures", IEEE Transactions on information technology in medicine, Vol.14, no 5, pp. 1197-1203, 2010.

[19] S.V.Bozhokin, S.V. Zharko, N.V.Larionov, A.N.Litvinov, I.M.Sokolov, "Wavelet Correlation of Nonstationary Signals", Technical Physics, Vol. 62, no 6, pp. 837-845, 2017.

[20] S.V.Bozhokin, "Continuous Wavelet Transform and Exactly solvable Model of Nonstationary Signals", Technical Physics, Vol. 57, no 7, pp. 900-906, 2012.

[21] D.A.Andreev, S.V.Bozhokin, I.D.Venevtsev, K.T.Zhunusov, "Gabor transform and continuous wavelet transform for model pulsed signals", Technical Physics, Vol. 59, no 10, pp. 1428-1433, 2014.

[22] S.V.Bozhokin, I.M.Suslova I.M., "Double Wavelet Transform of Frequency-Modulated Nonstationary Signal", Technical Physics, Vol. 58, no 12, pp. 1730-1736, 2013.

ISSN: 2319-5967
ISO 9001:2008 Certified
International Journal of Engineering Science and Innovative Technology (IJESIT)
Volume 7, Issue 1, January 2018

[23] S.V.Bozhokin, I.B.Suslova., "Wavelet-based analysis of spectral rearrangements of EEG patterns and of non-stationary correlations", Physica A: Statistical Mechanics and its Applications, Vol. 421, no 1, pp.151-160, 2015.

AUTHOR BIOGRAPHY

S.V.Bozhokin, Ph.D., Associated Prof. at the Department of theoretical physics, Peter the Great Saint-Petersburg Polytechnic University. Field of interests: theoretical physics, processing of nonstationary signals, biomedical signals processing.

I.B.Suslova, Ph.D., Associated Prof. at the Department of theoretical mechanics, Institute of Applied Mathematics and Mechanics, Peter the Great Saint-Petersburg Polytechnic University. Field of the research work: integral transforms and applications, biomedical signals processing.

D.E. Tarakanov, Ph,D. Peter the Great Saint-Petersburg Polytechnic University. Computer Science.